Acta Astronautica 177 (2020) 286–298

Contents lists available at ScienceDirect

Acta Astronautica

journal homepage: www.elsevier.com/locate/actaastro

ISRO's Unprecedented Journey to the Moon

Mathavaraj S *, Kuldeep Negi, Gaurav Vaibhav

Scientist, Trajectory Design & Analysis Section, Orbit Transfers Design Division, Flight Dynamics Group, U. R. Rao Satellite Center, Indian Space Research Organisation, Bangalore, India

ARTICLE INFO

Keywords:
Chandrayaan-2
Ground trajectory design
Target lunar orbit
Trans-lunar insertion
Lunar capture
Lunar orbit insertion
Lunar ground track acquisition
Powered descent phase
Indian Space Research Organisation (ISRO)

ABSTRACT

Chandrayaan-2, being the sequel of Indian Lunar Mission, differs with Chandrayaan-1 in targeting a specific lunar orbit. The primary ground trajectory design objective is to achieve the desired lunar orbit, from which the lander attempts soft-landing on the pre-selected landing site. The target lunar orbit is designed such that while landing, the Sun elevation rise angle is 6° on the desired site. This is to ensure the lander touchdown is close to sunrise, which in-turn will maximize the lander mission life to one lunar solar day (approximately 14 Earth days). This makes the Chandrayaan-2 trajectory design unique and challenging in itself. The maneuver strategy has been worked out to acquire the specific target lunar orbit. The objective of the powered descent phase is soft-landing over the desired site satisfying all the sensor constraints. This multi-phase lunar landing optimal control problem has been solved for trajectory design of the powered descent phase. Based on this design, the Chandrayaan-2 spacecraft has been launched on 22nd July, 2019 UT and successfully rendezvoused with the Moon on 20th August, 2019 UT and has attempted a soft-landing on 6th September, 2019 UT.

1. Introduction

Exploration of the Moon has attracted global attention [1] since it is found to be mineral rich [2]. Because of its proximity to Earth, the Moon is often favored as a base for conducting new demonstrations in space technology [3] like solar power harvesting [4]. Further, it can also act as a base [5] for launching ambitious missions to reach halo orbits around a Lagrangian point and extending human explorations to interplanetary destinations [6] such as Mars expeditions [7]. In addition, proof of existence of water on the Moon confirmed by the impact probe of the Chandrayaan-1 [8] has given enormous hope for assistance when an envisaged lunar research base is constructed on the surface of the Moon. The far side of the Moon [9] is away from Earth's radio signals hence its suitable for setting up cosmological bases [10]. Hence, there is a renewed interest across the globe for thorough exploration of the Moon in the near future.

Landing missions on celestial bodies without an atmosphere (such as the Moon, asteroid) demands meticulous planning and execution of engine burns [11]. In the literature, detailed analysis on lunar transfer trajectory design methodology has been documented [12–17]. In this paper, the target lunar orbit design methodology adapted for the Chandrayaan-2 mission has been explained in detail along with the mission constraints. This paper also summarizes the details of the executed maneuvers and the post realized orbits in Earth as well as Moon bound phase during Chandrayaan-2 landing mission. It is to be noted that though the lander hard landed on the moon's surface, the landing orbit prior to the attempt was achieved successfully. This paper will give a methodology to achieve the target lunar orbit for landing that can be useful for any other future attempts.

2. Chandrayaan-2 spacecraft

Chandrayaan-2 is configured as a composite module system comprising of an Orbiter Craft (OC) and Lander Craft (LC) named *Vikram* [18], with a six wheel rover named *Pragyan* accommodated inside *Vikram*. The OC and LC modules are interfaced mechanically by an inter module adaptor. The stowed configuration of the Chandrayaan-2 stack is shown in Fig. 1. The orbiter has bi-propellant (MMH+MON-3) propulsion system using one 440 N liquid engine. To determine the attitude of the spacecraft, the OC is equipped with two MK-II star sensors [19]. The OC also has Li-Ion battery with two solar panels for power generation.

Vikram has bi-propellant (MMH+MON-3) propulsion system using four 800 N throttleable engines as well as one central fixed thrust liquid engine for velocity reduction while landing and eight 58 N reaction control system thrusters for controlling the attitude. It is also equipped with four reaction wheel, Li-Ion battery with body mounted solar panel. The sensors available in *Vikram* are Laser Inertial Referencing and Accelerometer Package (LIRAP), Ka-Band Altimeter (KaRA), Lander Horizontal Velocity Camera (LHVC), Lander Position Detection Camera

* Corresponding author.
E-mail address: mathan.hce@gmail.com (S Mathavaraj).

https://doi.org/10.1016/j.actaastro.2020.07.046
Received 20 January 2020; Received in revised form 30 June 2020; Accepted 28 July 2020
Available online 3 August 2020

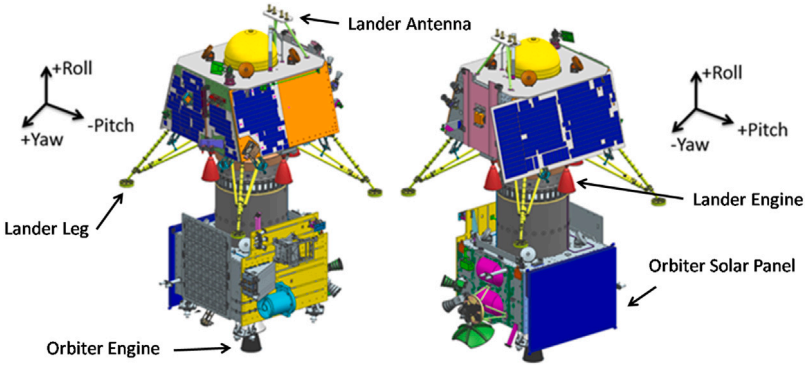

Fig. 1. Isometric view of the Chandrayaan-2 spacecraft (stowed configuration).

(LPDC), Lander Hazard Detection & Avoidance Camera (LHDAC), Laser Altimeter (LASA), Micro Star sensor, Inclinometer, Touchdown sensors. For more details on the working principle of these sensors, interested reader can refer to [18].

The attitude and orbit control subsystem (AOCS) of the Chandrayaan-2 (orbiter as well as lander) is configured as a three axis body stabilized zero momentum system with reaction wheels to provide a stable platform. The attitude and orbit control electronics (AOCE) receives the attitude data from the star sensors, body rates data from the gyro and then computes the necessary control torque commands and outputs to the actuators.

The functional requirements of AOCS and AOCE are

(i) Satellite three axis attitude acquisition
(ii) Maintaining attitude definitions during different phases of the trajectory
(iii) Orbital maneuvers for Earth bound, transfer trajectory, LOI insertion, Moon bound, orbit maintenance, powered descent phase
(iv) Attitude maneuvers for reorientation during orbital maneuvers
(v) Fault detection isolation and reconfiguration of actuators, sensors and reaction control system
(vi) Safe mode detection and recovery using master recovery scheduler
(vii) Autonomous execution of liquid engine burns
(viii) Attitude maneuver required for payload imaging
(ix) Automated momentum dumping
(x) Dual gimbal antenna motor tracking
(xi) Coarse analog Sun sensor acquisition while encountering safe mode operation

For more details on spacecraft dynamics and control, one can refer to [20].

As the spacecraft carries various payloads and sensors, it becomes necessary to perform the calibration for each element before actual commissioning of these systems. During Chandrayaan-2 mission, following calibration activities are carried out

(i) Star sensor relative alignment. This operation is carried out in Earth phase after injection.
(ii) Orbiter gyro scale factor, misalignment, drift estimation. This operation is carried out in Earth phase after injection.
(iii) Lander gyro scale factor, misalignment, drift estimation. This operation is carried out in Earth phase as well as in lunar phase.
(iv) Orbiter–Lander alignment angles. This operation is carried out in Earth phase after injection.
(v) Accelerometer calibration for orbiter as well as lander craft. This operation is carried out in Earth phase as well as in lunar phase.
(vi) Payload calibrations. This operation is carried out in Earth phase as well as in lunar phase depending on the payload specification.
(vii) SRP acceleration and torque estimation. This operation is carried out in Earth phase after injection as well as in lunar phase.
(viii) Radio frequency chain tests. This operation is carried out in Earth phase after injection.

Chandrayaan-2 mission is designed to expand the lunar scientific knowledge through detailed study of topography, seismography, mineral identification and its distribution, surface chemical composition, thermo-physical characteristics of top soil, composition of tenuous lunar atmosphere and so on leading to new understanding of the origin and evolution of Moon. In order to carry out these experiments the spacecraft has been equipped with various payloads. The orbiter craft consists of following payloads:

(i) Chandrayaan-2 Large Area Soft X-ray Spectrometer (CLASS)
It maps the abundance of the major rock forming elements such as Mg, Al, Si, Ca, Ti and Fe on the lunar surface at a spatial resolution on 12.5 km using the technique of X-ray fluorescence.
(ii) X-ray Solar Monitor (XSM)
It observe the X-rays emitted from the Sun as well as the Sun corona. It also supports the CLASS payload observation.
(iii) Dual Frequency Synthetic Aperture Radar (SAR)
It observers the scattering characteristics of lunar surface and sub-surface features which aid to mapping the lunar craters, boulders, especially in the polar regions.
(iv) Imaging IR Spectrometer (IIRS)
It images the Moon surface in 0.8 to 5 micron spectral region to investigate and identify the minerals. It also used in detection of signatures of hydroxyl (OH) and water (H2O) molecules in the polar regions.
(v) CHandra's Atmospheric Composition Explorer (CHACE)
It has neutral mass spectrometer which will carry out a detailed study of the lunar exosphere.
(vi) Terrain Mapping Camera (TMC)
It has three cameras — fore, nadir and aft. It has resolution of 5 m with swath of 20 km. It helps in generating a detailed three dimensional map of the lunar surface.
(vii) Dual Frequency Radio Science Experiment (DFRS)
It is used to measure the total electron content of the lunar ionosphere and its morphology.
(viii) Optical High Resolution Camera (OHRC)
It helps in generating high resolution image of the landing site. It has a resolution of 0.32 m which will be used during powered descent phase for pinpoint landing.

The lander craft - *Vikram* has following payloads:

(i) Radio Anatomy of Moon Bound Hypersensitive ionosphere and Atmosphere (RAMBHA)
It is used to measure the near surface plasma density of ions and electrons and its changes with respect to time.
(ii) Chandra's Surface Thermo physical Experiment (ChaSTE)
It is used to analyze the thermal properties of lunar surface near the polar regions.

Acronyms

AOCE	Attitude and Orbit Control Electronics
AOCS	Attitude and Orbit Control Subsystem
AOP	Argument Of Perigee
DEO-1	Deorbit 1
DEO-2	Deorbit 2
DTM	Drag Temperature Model
EBA	Earth Bound Apogee Maneuver
EBN	Earth Bound Maneuver
EME $J2000$	Earth Mean Equator and Equinox at 12 : 00 Terrestrial Time on 1 January 2000
EPO	Elliptical Parking Orbit
GSLV	Geosynchronous Satellite Launch Vehicle
GT	Ground Track
IAU	International Astronomical Union
IDSN	Indian Deep Space Network
ISRO	Indian Space Research Organisation
JPL	Jet Propulsion Laboratory
KaRA	Ka-Band Altimeter
LASA	Laser Altimeter
LBN	Lunar Bound Maneuver
LC	Lander Craft
LHDAC	Lander Hazard Detection & Avoidance Camera
LHVC	Lander Horizontal Velocity Camera
LIRAP	Laser Inertial Referencing and Accelerometer Package
LOI	Lunar Orbit Insertion
LPDC	Lander Position Detection Camera
LTT	Lunar Transfer Trajectory
LVLH	Local Vertical Local Horizontal
MCMF-PA	Moon Centered Moon Fixed - Principal Axis
MVR	Maneuver
NLP	Nonlinear Programming Problem
OC	Orbiter Craft
OHRC	Optical High Resolution Camera
PD	Powered Descent
Pragyan	Rover
RAAN	Right Ascension of Ascending Node
S/C	Spacecraft
SDSC	Satish Dhawan Space Centre
SOI	Sphere Of Influence
T.C.	Terminal Condition
TCM	Trajectory Correction Maneuver
TLI	Trans Lunar Injection
UT	Universal Time
UH 25	75% unsymmetrical dimethylhydrazine and 25% hydrazine hydrate
Vikram	Lander Craft

(iii) Instrument for Lunar Seismic Activity (ILSA)
It is used to measure the seismic activity around the landing site and also used in delineating the structure of the lunar crust and mantle.

(iv) Laser Retro reflector Array (LRA)
It has an array of mirrors that provide a target for laser tracking measurements from the ground. It is a passive payload from NASA - JPL.

The rover - *Pragyan* has following payloads,

(i) Laser Induced Breakdown Spectroscope (LIBS)
It performs qualitative and quantitative elemental analysis on the lunar surface. It is used to derive the chemical and mineralogical composition which gives in-depth understanding of the lunar surface around the lunar landing site.

(ii) Alpha Particle X-ray Spectrometer (APXS)
It is used to determine the elemental composition such as Mg, Al, Si, K, Ca, Ti, Fe of the lunar soil around the lunar landing site.

For more details on the technological specification of these payloads, one can refer to [21].

3. Chandrayaan-2 mission constraints

Chandrayaan-2, being the sequel of Indian Lunar Mission, differs with Chandrayaan-1 [22] in targeting specific lunar orbit. The objective of the trajectory design is to transfer the spacecraft from the Earth elliptic parking orbit (EPO) to Moon's target orbit around the Moon and followed by the design of the powered descent trajectory for soft-landing. The target lunar orbit to be achieved is a polar, near circular orbit passing through the desired site when sunrise happens. The trajectory design is carried out to meet the following constraints:

(i) While landing, the Sun elevation rise angle at landing site should be greater than 6°. It satisfies two constraints (i) Eight hours before powered descent start, the landing site should be imaged under proper illumination using OHRC payload (ii) after touchdown the lander should produce power from the body mounted solar panels. *This constraint is achieved by target lunar orbit design which in-turn realized by ensuring specific trans-lunar departure condition.*

(ii) During powered descent phase initiation, the lunar orbit should be polar i.e. the inclination is 90° which leads to negligible cross axis ground track shift. This constraint also gives the ability to image the entire lunar surface using the orbiter payloads throughout its mission life. *This constraint is achieved by ensuring specific trans-lunar departure condition.*

(iii) Lander should spend over 3 days in the near 120×30 km lunar orbit for calibration of *Vikram* systems as well as for orbit determination and powered descent trajectory design. *This constraint is achieved by appropriate selection of (i) separation epoch (ii) Deorbit-1 (DEO-1) epoch, burn orientation (iii) Deorbit-2 (DEO-2) epoch, delta-V and burn orientation.*

(iv) Post LC-OC separation, acquire landing site in *Vikram* ground trace. *This constraint is achieved by appropriate design of DEO-1 and DEO-2.*

(v) Post LC-OC separation, acquire landing site in orbiter ground trace. *This constraint is achieved by appropriate design of orbiter ground track acquisition maneuver.*

(vi) Obtain minimum eclipse duration in composite lunar orbit phase. This requirement is driven by orbiter as well as lander battery capacity to support the spacecraft during Moon's shadow over it. *This constraint is achieved by target lunar orbit design* discussed in Section 4.

(vii) The ground stations which are available for the Chandrayaan-2 mission are Madrid, Goldstone, Canberra, IDSN-32, IDSN-18, Bangalore, Mariti, Biak, Lucknow, Brunei, Alcantara, Cuiaba, Hartebeesthoek. The trajectory should be designed such that the burns are visible with either of these stations. *This constraint is achieved by orbit sizing which is realized by imparting appropriate ΔV in each burn.*

(viii) Minimize the total delta-V expenditure for lunar orbit acquisition which in turn reduces the propellant expenditure, subsequently enhancing the mission life of the orbiter. *This constraint is achieved by ensuring near perigee burns as well as by minimizing the out-of-plane maneuvers to achieve the target orbit.*

In order to realize these mission constraints, the Earth to Moon transfer trajectory is comprised of the following phases:

1. Earth phase
2. Lunar transfer trajectory (LTT) phase
3. Lunar phase

The spacecraft is injected into an elliptic parking orbit by the launcher. The apogee of the elliptical parking orbit is raised by Earth bound perigee burns (Earth phase) to reach the Moon's orbit around the Earth. Note the final Earth burn, i.e. trans lunar injection (TLI) pushes the spacecraft into lunar transfer trajectory (LTT phase) which rendezvous with the Moon. The spacecraft arrives at the Moon's sphere of influence (SOI) in a hyperbolic trajectory with respect to the Moon. The sphere of influence of Moon is given by the radius within which the primary gravitational acceleration is due to the Moon and the acceleration due to Earth and other celestial bodies are considered as a perturbing acceleration. After the spacecraft enters the Moon's SOI, the Moon becomes the primary body for spacecraft and hence the inertial axis for state propagation is shifted to Moon's center. The Moon's SOI is about $66,000$ km from Moon's center. When the spacecraft reaches the closest to Moon (periselene), the spacecraft is captured around Moon with the lunar bound periselene maneuver (lunar phase).

At the closest approach to the Moon's surface, lunar orbit insertion maneuver is planned. As the incoming trajectory to Moon is hyperbolic orbit, there is need for velocity braking in order to be captured by Moon. After the lunar orbit insertion, the orbit is near polar elliptical orbit. Further lunar bound periselene maneuvers are carried out to make the capture orbit as near circular 120 km polar orbit.

Vikram will be separated from OC at the appropriate time from the near circular 120 km lunar orbit. Subsequently with a time gap of approximately 18 h, a DEO-1 as well as DEO-2 maneuver is carried out on the LC to achieve a near 120 × 30 km orbit. *Vikram* will coast in this elliptical orbit for around 3 days to acquire the desired powered descent initial conditions. At this point, the powered descent will begin to achieve the soft-landing on the desired target site.

For the Chandrayaan-2 lunar landing mission, two desired sites in MCMF-PA frame [23] have been selected. One is the prime site which is at the latitude: 70.90°S, longitude: 22.78°E and the other one is the back-up site which is at the latitude: 67.75°S, longitude: 18.47°W. Back-up site is located approximately 38 ground trace paths (i.e. 3 days) away in the target lunar orbit towards the western side of prime site. The landing sites for the Vikram have been selected from an extensive study of the lunar images available from Chandrayaan-1 and Lunar Reconnaissance Orbiter spacecrafts based on the following reasons (i) remarkably free from boulders and craters in an area of 500 m × 500 m (ii) the achieved target lunar orbit for the prime landing site should also pass through the back-up site after 3 days (iii) the science exploration at the south pole.

4. Target lunar orbit design

It is to be noted that one solar day of Moon's is approximately 14 Earth days. If the lander lands on the desired site closer to sunrise, the lander has the ability to generate power for the subsequent 13 Earth days. This ensures maximum mission life for the lander. In addition, 4 orbits before powered descent phase, the desired site is imaged for high resolution images using OHRC payload which necessitates that the site should be well-illuminated. For the desired landing site (Latitude: 70.90°S, Longitude: 22.78°E), the epoch at which the sunrise (elevation angle 6°) is tabulated in Table 1. During landing, the orbital plane of the spacecraft should pass through the desired site at this epoch.

The objective is to find the spacecraft orbital plane parameters in Moon centered International Astronomical Union (IAU) inertial frame, which satisfies the sunrise constraints on the desired site. The IAU frame is intended for applications within the framework of *General Relativity*. The reference axis XYZ in Moon centered IAU frame has been defined by International Astronomical Union (IAU) [24]. Out of six orbital parameters, the right ascension of ascending node (RAAN) is the key orbital element which aids in satisfying the sunrise constraints. The other orbital parameters namely semi-major axis, inclination, argument of perigee are similar for every landing opportunity since the desired orbit is elliptical 120×30 km polar orbit.

Table 1
Optimal RAAN requirement for desired landing site.

Landing date (UT)	Optimal RAAN required (deg)
2019 – 06 – 09, 23 : 00	190.0
2019 – 07 – 09, 14 : 00	220.0
2019 – 08 – 08, 05 : 00	251.0
2019 – 09 – 06, 19 : 00	280.0
2019 – 10 – 06, 09 : 00	310.0
2019 – 11 – 04, 21 : 00	339.0
2019 – 12 – 04, 07 : 00	6.5

From the definition of sidereal angle and RAAN, the necessary calculations are carried out. For a given epoch in Table 1, the sidereal angle θ_R of the Moon fixed principal x axis (like Greenwich in Earth centered Earth fixed frame) with respect to the IAU frame is calculated from the JPL ephemeris [25]. It is to be noted that the JPL ephemeris accounts for Moon's libration. The longitude of any site on Moon θ is defined with respect to the Moon fixed principle x axis frame (like longitude with respect to Greenwich). So the sidereal angle of the desired site θ_S in IAU frame is calculated as

$$\theta_S = \theta_R + \theta \tag{1}$$

So if the RAAN of the lunar target orbit matches the sidereal angle of the desired site θ_S, then the spacecraft orbit will pass through the desired site at the desired illumination epoch. Using this procedure, for the month July–December 2019, the required RAAN values in IAU frame is calculated and tabulated in Table 1.

5. Launch vehicle constraints

Chandrayaan-2 is launched using the Geosynchronous Satellite Launch Vehicle (GSLV) Mark III [26,27] into an Earth elliptic parking orbit (EPO). Next, the orbiter propulsion system is used to carry the lander till near 120 km circular lunar polar orbit. Successively, the lander is de-orbited to elliptical orbit of near 120×30 km using its own propulsion system. Out of all ISRO launch vehicles, GSLV Mark III is selected because of its higher liftoff capacity.

The GSLV Mark III vehicle is a three stage heavy lift launcher capable of injecting 4 ton class payloads into geo-synchronous transfer orbit (GTO) when launched from SDSC, Sriharikota [28]. In GSLV Mark III vehicle, the $L110$ liquid stage is the core booster which functions as the second stage with the two $S200$ solid strapons forming the first stage. The final upper stage is a cryogenic $C25$ stage with 25 ton of useful propellant. GSLV Mark III also includes vehicle equipment bay and encapsulated assembly. $S200$ stage is a solid propellant booster using hydroxyl-terminated polybutadiene formulation with a nominal propellant loading of 200 ton. Here, the two $S200$ motors are mounted symmetric to the central core. Attitude control of the vehicle in the $S200$ firing regime is provided by the flex nozzle control system. $L110$ stage uses high thrust Vikas engines with propellant combination of UH 25 and dinitrogen tetroxide (N_2O_4). UH 25 is a mixture of 75% unsymmetrical dimethylhydrazine and 25% hydrazine hydrate. The vehicle attitude control in $L110$ regime is by engine gimbal control system. The final $C25$ stage uses cryogenic engine which provides a nominal thrust of 200 kN. The control system for the $C25$ stage is by electro-mechanical actuators, which provide pitch and yaw control and by reaction control system, which provide roll control. It has to be

Table 2
Different GSLV Mk III EPO Scenarios for 3850 kg Liftoff Mass.

AOP (deg)	Apogee height (km)	Perigee height (km)	Inclination (deg)
178.0	39350.9	170.0	21.5
198.0	35770.0	170.0	41.8
203.0	33925.0	170.0	41.8

Table 3
Moon's Orbit Equatorial Crossings.

Ascending node epoch (U T)	Radius (km)	Descending node epoch (U T)	Radius (km)
2019 – 06 – 26, 03 : 31	399646.150	2019 – 07 – 09, 03 : 20	371860.518
2019 – 07 – 23, 11 : 09	402193.722	2019 – 08 – 05, 09 : 53	366861.645
2019 – 08 – 19, 17 : 14	404117.285	2019 – 09 – 01, 18 : 27	361337.760
2019 – 09 – 15, 22 : 35	404516.205	2019 – 09 – 29, 04 : 50	358965.669
2019 – 10 – 13, 04 : 34	403674.723	2019 – 10 – 26, 15 : 34	361344.690
2019 – 11 – 09, 12 : 03	402706.144	2019 – 11 – 23, 00 : 41	366759.360
2019 – 12 – 06, 20 : 44	402642.739	2019 – 12 – 20, 07 : 18	370742.106

noted that $S200/L110$ stages are provided with independent destruct system to carry out remote destruction of the stage in case the vehicle deviates beyond the desired trajectory limits.

GSLV Mark III launch vehicle has the ability to provide different elliptic parking orbit options (i.e., different argument of perigee (AOP) values) for the same injection mass. As a case study, liftoff mass of 3850 kg is considered and the corresponding GSLV EPO options are tabulated in Table 2. It is to be noted that the EPO inclinations are different since the launch azimuths differ for each of these cases. The apogee altitude of the EPO decreases as the AOP increases from 178°. The reason is that the Earth rotational velocity is aiding for AOP 178° (inclination 21.5°) case compared to AOP 203° case (inclination 41.8°). Note that the permitted inclinations 21.5° and 41.8° are due to range safety constraints. So the optimum GSLV launch scenario for same injection mass is where the maximum apogee height is achieved i.e. the case where AOP is 178°. To achieve the target lunar orbit RAAN requirement for each month as given in Table 1, there is a specific AOP requirement from the GSLV launch vehicle (discussed in Section 6). So it is preferable to choose a landing month in a year where the injection orbit of AOP 178° is able to capture the target lunar orbit.

6. Chandrayaan-2 launch opportunities

The Moon's orbit around the Earth has a orbital period of 27.3 Earth days during which two nodal crossings, ascending and descending, occur. Table 3 provides the epoch of the Moon's nodal crossings for the months of July–December 2019. This table also contains the separation distance between the Earth and Moon during these epochs. It varies over these months since Moon's orbit have a small eccentricity. It is to be noted that in year 2019, the Moon's orbit inclination with Earth's equator varies from 21.5° to 23.0°. The variation of the Moon's orbit inclination with respect to the Earth's equatorial plane is caused by the precession of the Moon's orbit plane which has a periodicity of about 19.6 years. The lunar orbit insertion (LOI) of the spacecraft around Moon is designed to happen close to the apogee of the Earth parking orbit. Hence, the GSLV injection orbit's apogee is raised till it reaches Moon's orbit i.e. approximately 400,000 km using the Earth bound perigee maneuvers.

Considering the apogee raise maneuver scenario and the geometry of the optimum GSLV elliptical parking orbit (AOP 178°), the spacecraft is possible to rendezvous with the Moon only twice in 27.3 days cycle. One opportunity comes closer to ascending node and the next opportunity comes closer to descending node in one full Moon's cycle. This results in a year, nearly 24 opportunities i.e. approximately two per month are the possible scenarios for capturing the Moon using

Table 4
Different Landing Opportunities for Jul-Dec 2019.

Launch Date (2019)	GSLV EPO (HP ×HA (km), AOP, Inclination)	TLI date (2019)	LOI Date (2019)	Landing Date (2019)
10th May	169 × 33925, 203°, 41.8°	02nd June	07th June	09th July
16th June	170 × 35770 198°, 41.8°	02nd July	06th July	08th Aug
09th July	170 × 39350 178°, 21.5°	31st July	05th Aug	06th Sep
18th July	170 × 39350 178°, 21.5°	13th Aug	19th Aug	06th Sep
23rd Aug	170 × 35770 198°, 41.8°	14th Sep	19th Sep	04th Nov
19th Sept	170 × 35770 198°, 41.8°	11th Oct	16th Oct	04th Nov

Earth bound perigee maneuvers. It is to be noted that several opportunities are possible every month for target lunar orbit acquisitions if corresponding desired AOP are achieved during TLI departure. These desired AOP are achievable by two ways — either the launch vehicle injects the spacecraft with the desired AOP or the satellite injected from the launch vehicle achieves the desired AOP using its propellant. As discussed in Section 5, the EPO apogee height reduces, if the launch vehicle deviates from the optimum AOP case, resulting in additional propellant consumption to increase the apogee height. Since both of these methodology penalizes the spacecraft mission life, such scenarios are not recommended for the Chandrayaan-2 mission.

In this context, for achieving the target lunar orbit (desired RAAN and inclination), the sensitivity analysis was carried out considering the various GSLV-EPO options (refer to Table 2) by varying TLI time and delta-V. Table 4 provides various launch opportunities using GSLV Mark III launch vehicle to achieve the target RAAN for the month of July–December 2019. It is to be noted that landing on October as well as December 2019 is not desired because the required AOP for these months is not within the capability of GSLV Mark III. In general, all these launch dates have one week of launch period holding the same TLI date, which is achievable by modifying the orbital period of each Earth bound orbits.

7. Trajectory modeling and determination

During Chandrayaan-2 mission, based on the different phase of the trajectory, various force models are considered. Force model considered during Earth bound phase:

(i) Gravity model - GGM02C (100 × 100)
(ii) Atmospheric drag temperature model (DTM) [29]
(iii) Spherical and/or variable area drag model
(iv) Flat plate and/or variable area solar radiation pressure model
(v) Sun, the Moon and other planets as third body
(vi) Coordinate frame considered for the analysis is Earth centered EME $J2000$

Force model considered during Moon bound phase:

(i) Gravity model – GRAIL900C (150 × 150)
(ii) Flat plate and/or variable area solar radiation pressure model
(iii) Sun, Earth and other planets as third body.
(iv) Coordinate frame considered for the analysis is Moon centered EME $J2000$

Orbit determination is a process in which the model parameters are adjusted for converging to a best fit trajectory i.e., a trajectory for which the measurement residuals (difference between actual and the model predicted value) are smallest. Orbit determination process relies on weighted least square method. The estimated parameters are position and velocity, station biases, solar radiation pressure scale factor,

momentum dumping scale factor. The fundamental requirements for the orbit determination process are measurements, tracking network and modeling.

7.1. Measurements

Tracking station on the Earth are used to send the signals which are used for communication with the spacecraft. From these signals, there are three basic type of observations — time delay, phase delay and angles. From these basic observations — range, range rate, angles and difference of range measurement are derived for orbit determination. In general, a deep space mission commonly uses Doppler and range data measurements.

7.2. Tracking network

For the Chandrayaan-2 spacecraft orbit determination S-band tracking data are used. The network of stations utilized for the Chandrayaan-2 mission are

(i) Up to range of 100,000 km: Bangalore, Mariti, Biak, Lucknow, Brunei, Alcantara, Cuiaba, Hartebeesthoek
(ii) More than range of 100,000 km: Madrid, Goldstone, Canberra, IDSN-18, IDSN-32

7.3. Modeling of orbit determination system

Orbit determination system involves dynamic modeling as well as measurement modeling for the estimation process.

7.3.1. Dynamic modeling

The dynamic model which governs the equation of motion of the orbiting spacecraft, has following capability build within

(i) Central gravitational potential acceleration of the Earth, the Moon, Sun as well as other planets
(ii) Gravitational model of the Earth up to degree and order of 100
(iii) Gravitational model of the Moon up to degree and order of 150
(iv) Acceleration due to solar radiation pressure
(v) Acceleration due to air drag using DTM and JACHIA model [30]

For more details on dynamic modeling, interested reader can refer to [12].

7.3.2. Measurement modeling

In general, the measurements received are corrupted due to various practical problems such as atmosphere attenuation, hardware delays and so on. In order to address these concerns, measurement corrections are adapted in the tracking data pre-processing. Tracking data pre-processing is an important procedure to be followed in orbit determination. The tracking data pre-processing access the raw data files that are retrieved from the tracking system of a particular ground station and documents the measurement along with auxiliary information related to them into the observation file which is suitably formatted for orbit determination. For orbit determination of the Chandrayaan-2 spacecraft, the following data types are used.

(i) Two way range data
(ii) Two way Doppler data
(iii) Angles

Essentially, the tracking data comprises of range data, Doppler data and mechanical angle data i.e., azimuth and elevation of the ground station antenna with respect to the satellite. However, the angle measurement does not help in the improvement of orbit determination accuracy of range and Doppler. However, it helps in contingency scenarios, to get the initial orbit determination. Next, measurement corrections are adapted in the tracking data pre-processing for addressing the following parameters:

Table 5
Achieved GSLV elliptical parking orbital characteristics. Lift-off Epoch (UT): 2019-07-22 09:29:45.840.

EPO Parameter	Value
Semi-major axis (km)	29182.00
Eccentricity	0.7756
Inclination (deg)	21.46
Argument of perigee (deg)	178.08
Right ascension of ascending node (deg)	18.07
Mean anomaly (deg)	0.51
Orbit period (hrs)	13.78

(i) The refraction of signal when passing through the Earth troposphere and ionosphere
(ii) Instrumental delays in the spacecraft and/or the ground stations
(iii) Newtonian light time i.e., the light time needs to travel on straight line

For more details on measurement modeling, interested reader can refer to [31].

8. Composite module trajectory design

Based on the launch opportunities discussed in Section 6, the launch dates have been selected depending on the spacecraft readiness. At first, 14th July 2019 UT was selected for launch which has TLI date on 31st July 2019 UT. This launch scenario has optimal AOP of 178° (refer to Table 4) resulting in the maximum apogee height provided by launch vehicle. The spacecraft had been shipped to SDSC, Sriharikota [28] and the countdown was initiated for launch. However, due to technical glitch in the GSLV Mark III a prior liftoff, the launch was called off. Since the GSLV glitch was minor, the next possible launch opportunity i.e., 22nd July 2019 UT has been selected for the launch which also has optimum AOP of 178° (refer to Table 4). Chandrayaan-2 spacecraft has been successfully injected by GSLV Mark III and the achieved elliptical parking orbital characteristics is tabulated in Table 5. It is to be noted that achieved apogee height is approximately 6000 km more than nominal value because of the depletion mode operation of the launch vehicle. Due to the off-nominal EPO apogee height, nominal design of 6 Earth bound perigee burn, which is planned to raise the apogee, has been reduced to 5 Earth bound perigee burn strategy. However, the increased EPO apogee height has resulted in the orbiter propellant saving which increased its mission life from 1 yrs to 2 yrs approximately. After injection from the launch vehicle, the orbital period of the EPO orbit is 13.8 h.

In total, six Earth bound maneuvers — one apogee maneuver and 5 perigee maneuvers are planned as given in Table 6 in which the last EBN is Trans Lunar Injection (TLI) burn. The Earth bound apogee maneuver (EBA-1) is planned to raise the perigee of the parking orbit. Whenever the spacecraft passes through the EPO perigee of around 170 km, the spacecraft attitude gets disturbed because of the atmospheric drag torque. Hence, an apogee maneuver has been executed to increase the perigee height to 232 km. Then the subsequent Earth bound maneuvers (EBN) are executed to increase the apogee height of the orbit using Hohmann transfer [32,33] principles. It is to be noted that delta-V imparted in every burn has been selected such that appropriate orbital period after each burn is achieved which in-turn assures two things. Firstly, at every perigee burn, station visibility are available for telecommand and telemetry. Secondly, if any EBN abort scenario happens, there is sufficient time for subsequent EBN burn's adjustment so that the crucial TLI burn does not get changed.

The EBN maneuver orientation is constructed such that the roll is along the velocity vector (accelerating), pitch is along the negative orbit normal and yaw constructs the triad in the Earth centered EME $J2000$ frame. All the EBNs are planned with appropriate burn offset from the perigee as tabulated in Table 6, to capture the target lunar

Table 6
Realized Earth burn maneuvers summary.

MVR	No.	Burn start time (UT)	Burn duration (sec)	delta-V (m/s)	Burn offset (sec)
Injection	Perigee 01	2019 – 07 – 22, 09 : 29	–	–	–
EBA-1	Apogee 04	2019 – 07 – 24, 09 : 22	48.0	5.1	0.287
EBN-1	Perigee 07	2019 – 07 – 25, 19 : 38	882.6	99.4	440.0
EBN-2	Perigee 12	2019 – 07 – 29, 09 : 42	989.5	115.1	120.0
EBN-3	Perigee 16	2019 – 08 – 02, 09 : 58	646.2	77.5	120.0
EBN-4	Perigee 19	2019 – 08 – 06, 09 : 35	1040.8	130.3	200.0
TLI	Perigee 22	2019 – 08 – 13, 20 : 51	1202.9	158.3	−284.5

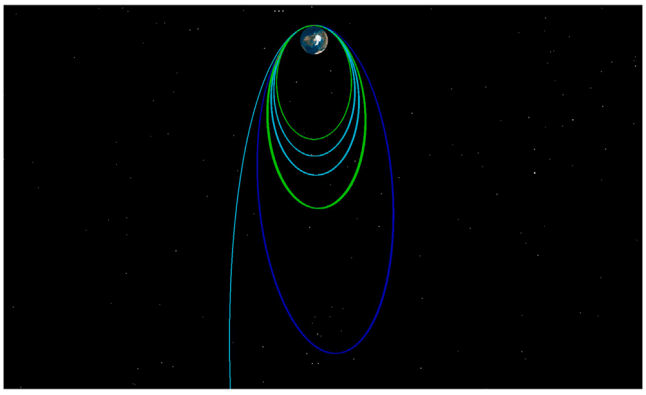

Fig. 2. Earth bound maneuvers including trans lunar insertion maneuver.

orbit. For EBN-4 maneuver alone, a yaw bias of 2° over the defined EBN maneuver orientation is executed. Table 6 gives the burn duration, delta-V in each burn during the EBN with time-line of the maneuver start. The overall burn duration is 4810.0 s which imparts delta-V of 585.7 m/s during Earth burns.

Table 7 provides the post EBN orbital parameters for each burn. Note the apogee altitude is increased gradually to 418223.3 km using the perigee maneuver, where the spacecraft rendezvous with the Moon. During the EBN, since most of the maneuvers are in-plane so there is no significant change in inclination except small changes due to the external perturbations. Due to the Earth oblateness, Sun's and Moon's gravitational pull and maneuver offset from perigee as well as bias, the AOP as well as RAAN of the orbit changes as specified in Table 7. The orbital period increases from 13.8 h to 276.9 h till TLI since semi-major axis is increasing after each EBN maneuvers. It is to be noted that each EBN burn (i.e., EBN-1 to EBN-4) execution errors are accommodated in the subsequent burn design itself. Fig. 2 shows the pictorial representation of the post orbital characteristics from EPO till TLI using the System Tool Kit [34].

After TLI, the spacecraft travels on the transfer trajectory towards the Moon. In this phase, sufficient data collection has been carried out for post TLI orbit determination and the achievable lunar orbit is calculated by full force model propagation. Though TLI maneuver execution errors are small, the deviations from the target lunar orbit is significant owing to the highly sensitive target lunar parameters. Hence, a trajectory correction maneuver (TCM-1) of 1.3 m/s is executed, within 48 h of post TLI, to achieve the desired target lunar orbit. It is to be noted that the spacecraft is still in Earth SOI during this phase. Hence, TCM-1 maneuver orientation is constructed in the similar fashion as EBN orientation with appropriate pitch and yaw bias as tabulated in Table 8. As soon as the spacecraft enters the Moon's SOI, the Moon becomes the primary body whereas the Earth gravitation acts as a major perturbing force on the satellite. Fig. 3 shows the all the Earth burns, TLI trajectory, Moon's orbit around Earth as well as lunar orbit insertion capture geometry.

As the incoming trajectory to Moon is hyperbolic orbit, there is need for braking the velocity in order to be captured by Moon. The lunar bound maneuver (LBN) maneuver orientation is constructed such that

Table 7
Post earth burn achieved orbital elements in EME-J2000 frame.

MVR	Prg Alt. (km)	Apg Alt. (km)	Incl (deg)	AOP (deg)	RAAN (deg)	Period (hrs)
Injection	169.7	45438.1	21.5	178.1	18.1	13.8
EBA-1	232.3	45161.2	21.5	179.1	17.5	13.7
EBN-1	256.7	54733.0	21.5	181.1	17.1	17.2
EBN-2	268.0	71553.7	21.5	182.4	16.3	24.0
EBN-3	277.9	89037.0	21.7	183.6	15.7	31.9
EBN-4	284.2	142275.7	21.7	184.8	15.3	60.2
TLI	336.0	418223.3	21.7	184.8	15.0	276.9

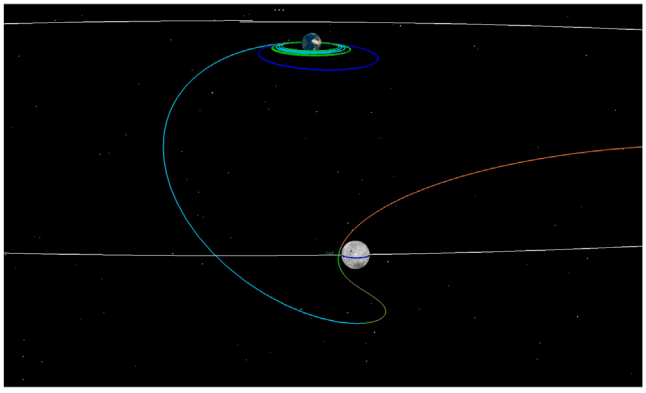

Fig. 3. Lunar orbit insertion maneuver along with Moon's orbit around Earth.

roll is along the negative velocity vector (decelerating), pitch is along the orbit normal and yaw constructs the triad in the Moon centered EME $J2000$. All the LBNs are planned with appropriate yaw as well as pitch bias as tabulated in Table 8 over the defined LBN maneuver orientation. The LBN maneuver start time-line, burn duration, delta-V has been tabulated in Table 8.

At the closest approach to the Moon's surface, lunar orbit insertion (LBN-1) braking maneuver is executed. The post LBN-1 orbit is near polar elliptical orbit with the periselene and aposelene height of around 150×18000 km orbit. It is to be noted that the LBN-1 epoch is close to the ascending node epoch of 19th August 2019 UT (refer to Table 3) as well as post LBN-1 achieved lunar IAU RAAN is 280.97° (refer to Table 9) leading to 06th September 2019 UT landing scenario (refer to Table 1). Further, four LBN maneuvers are performed to make the capture orbit a 120 km near circular orbit. The overall LBN burn duration is 5391.3 s which imparts delta-V of 834.0 m/s.

After each LBN, the post orbital parameters are tabulated in Table 9. As explained earlier, the braking maneuver reduces the periselene and aposelene height close to 120 km. It is to be noted that post LBN-5 the achieved RAAN is 279.97° which satisfies the 2019 September month landing requirement. Hence, the orbit will pass over the landing site close to epoch 2019-09-06, 19 : 00 UT during which Sun illumination is greater than 6°.

As the semi-major axis is reduced during each LBN burns, the orbital period reduces from 28.0 h to 2.0 h. Due to the Sun's and Earth's gravitational pull on the spacecraft, the inclination varies around 90°

Table 8
Realized TCM-1 and lunar burn maneuvers summary.

MVR	Prg No.	Burn start time (UT)	Burn duration (sec)	delta-V (m/s)	Pitch bias (deg)	Yaw bias (deg)
TCM-1	–	2019 – 08 – 15, 12 : 10	26.8	1.3	0.0	0.0
LBN-1	1	2019 – 08 – 20, 03 : 32	1738.4	246.6	0.0	0.0
LBN-2	2	2019 – 08 – 21, 07 : 21	1228.4	186.7	0.0	0.0
LBN-3	30	2019 – 08 – 28, 03 : 34	1189.8	191.5	0.0	0.25
LBN-4	48	2019 – 08 – 30, 12 : 48	1155.4	198.7	0.0	0.07
LBN-5	72	2019 – 09 – 01, 52 : 5	52.5	9.2	0.0	−1.4
Total			5391.3	834.0		

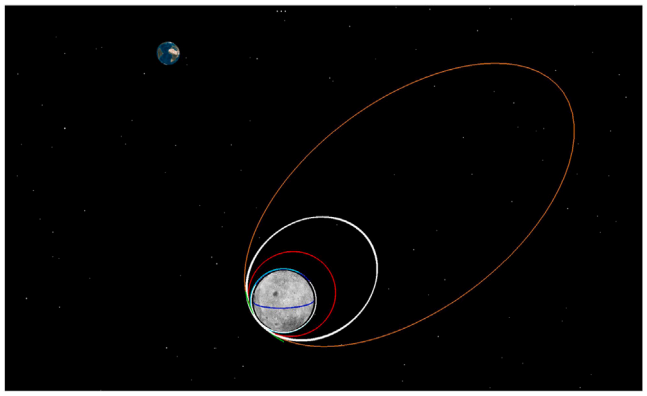

Fig. 4. Lunar bound maneuvers including lunar orbit insertion maneuver.

Table 9
Post TCM-1 and lunar burn achieved orbital elements in IAU frame.

MVR	Prs Alt. (km)	Aps Alt. (km)	Incl (deg)	AOP (deg)	RAAN (deg)	Period (hrs)
TCM-1	148.5	–	87.97	324.39	280.97	–
LBN-1	114.7	18036.2	87.94	323.82	280.97	28.0
LBN-2	118.4	4414.7	88.92	322.98	280.42	6.3
LBN-3	179.0	1413.8	89.54	322.28	280.08	3.2
LBN-4	124.9	164.6	89.17	161.71	280.08	2.04
LBN-5	119.5	127.1	88.89	328.17	279.97	2.00

during the lunar bound phase. At lower altitudes, the non-sphericity of the Moon also affect the achieved orbital parameters. Fig. 4 gives the pictorial representation of the LBN post orbital characteristics around the Moon. As shown, the incoming hyperbolic orbit is changed to elliptical Moon bound orbit by braking maneuver LBN-1 and then subsequently to near circular orbit by LBN-2, 3, 4, 5. In each LBN burn, delta-V has been selected to satisfy three criteria - (i) each LBN burn has station visibility for telecommand and telemetry (ii) if any LBN abort scenario occurs there is sufficient time for subsequent LBN's adjustment so that there is no change in the crucial de-orbit strategy (iii) the inclination during powered descent phase should satisfy $90° \pm 0.01°$.

The spacecraft mass as well as propellant consumed for orbiter craft has been tabulated in Table 10. Propellant of 656.32 kg and 747.48 kg has been consumed using the 440 N engine during the Earth bound phase and lunar bound phase respectively. However, the overall spacecraft mass reduction is not only due to periapse raise and apoapse raise maneuvers but also due to momentum dumping, achieving different target attitudes for various mission operations such as safe orientations, burn orientations, payload operation orientations and so on. Table 10 provides the spacecraft mass at the start of each burn. It is to be noted that since the Vikram lander gets separated post LBN-5, there is a drastic drop in the spacecraft mass a prior to the GT acquisition maneuver.

9. Vikram deorbit trajectory design

As per the above executed design, the spacecraft — orbiter and lander is orbiting around the Moon in the near circular polar 120 km orbit which will pass through the desired site at sunrise time. Following are the major successive operational sequences to satisfy the landing constraints:

1. Lander–orbiter module separation in the near circular 120 km orbit
2. De-orbit the lander from the circular orbit to near 120×30 km elliptical orbit
3. Initializing the powered descent at a specific position and epoch in the lander's elliptical orbit so that desired landing site is achieved while touch down

Table 10
Chandrayaan-2 orbiter propellant consumption summary.

MVR	Spacecraft mass (kg)	Propellant consumption due to 440 *N* (kg)
Injection	3846.05	–
EBA-1	3844.45	6.24
EBN-1	3835.46	120.40
EBN-2	3712.35	134.37
EBN-3	3573.40	87.71
EBN-4	3480.80	142.43
TLI	3336.07	165.17
TCM-1	3170.61	1.52
LBN-1	3169.01	241.15
LBN-2	2927.65	170.35
LBN-3	2757.50	164.68
LBN-4	2592.50	160.66
LBN-5	2431.29	7.15
GT Acquisition	946.90	1.97
Total		1403.80

These constraints resulted in four distinct phases that need to be realized in order to land the lunar module on to the surface of Moon. They are: (i) Separation phase (from orbiter) (ii) De-orbit maneuver phase (iii) Transfer orbit phase in 120 × 30 elliptical orbit and (iv) Powered descent phase.

Deorbit phase is to maneuver the lander from 120 km target orbit to reach 30 km altitude. The lander is designed to orbit for approximately three days in transfer orbit phase, with appropriate conditions for the lander to approach landing site when the powered descent phase is initialized. This is carefully planned such that re-targeting and out-of-plane maneuver that costs additional fuel consumption is avoided. The detailed timeline of this design is summarized in Table 11.

On 2nd September 2019 UT, *Vikram* has been separated from orbiter using spring mechanism which imparted delta-V of 0.3 m/s on the lander. Similarly orbiter has experienced delta-V of 0.4 m/s due to separation. During separation, there is requirement of two different ground antenna system for telecommand and telemetry i.e., one for lander and one for orbiter which calls for dual station visibility for this operation which is ensured by appropriate selection of separation epoch. The deep space station supported during LC-OC separation are IDSN-32 and Canberra. Next, as tabulated in Table 11, two de-orbit maneuvers are executed using the lander propulsion system. First de-orbit burn (DEO-1), in which testing of *Vikram* engines is the primary objective, has been executed on 3rd September 2019 UT. The sequences of the engine firing for DEO-1 is first one sec of central engine followed

Table 11
Finite lunar burn maneuvers.

MVR	Burn start time (UT)	S/C Mass (kg)	Burn duration (sec)	delta-V (m/s)	Propellant (kg)
Orbiter separation	2019 – 09 – 02, 07 : 45	946.90	–	0.5	–
Vikram separation	2019 – 09 – 02, 07 : 45	1477.27	–	0.3	–
Vikram DEO-1	2019 – 09 – 03, 03 : 20	1477.08	4.0	3.0	1.50
Orbiter GT acquisition	2019 – 09 – 03, 06 : 26	946.90	36.5	5.6	1.97
Vikram DEO-2	2019 – 09 – 03, 22 : 12	1475.06	9.1	21.2	11.3

Table 12
Finite lunar burn parameters in IAU frame.

MVR	Prs Alt. (km)	Aps Alt. (km)	Incl (deg)	AOP (deg)	RAAN (deg)	Period (hrs)
Orbiter separation	117.3	130.4	88.89	325.76	279.95	2.00
Vikram separation	117.6	127.9	88.89	336.54	279.96	2.00
Vikram DEO-1	100.1	130.8	89.14	24.104	280.07	1.99
Orbiter GT acquisition	97.2	125.3	89.05	276.78	279.98	1.98
Vikram DEO-2	36.1	101.3	89.15	231.14	280.07	1.91

by one sec of two diagonal engines and then one sec of opposite diagonal engines. DEO-1 has reduced the periselene altitude from 117.6 km to 97.2 km as tabulated in Table 12. Second de-orbit maneuver (DEO-2) objective is to achieve the desired powered descent initial condition. In DEO-2, the sequence of engine firing is one sec of central engine following by all 5 engines of *Vikram*. DEO-2 is scheduled such that 3 days later, landing site will be acquired for powered descent phase. DEO-2 has been executed to reduce the periselene height to 36.1 km so that after three days of orbiting around Moon, the periselene height reduces to near 30 km due to external perturbation forces. For orbiter, ground track acquisition maneuver is carried out on 3rd, September 2019. This maneuver is executed (refer to Table 11) for achieving the desired condition required for OHRC imaging operation of the landing site.

Approximately 18 h, from LBN-5 to separation, from separation to DEO-1 and from DEO-1 to DEO-2 has been maintained to ensure availability of sufficient time for orbit determination as well as for maneuver planning. If DEO-2 is missed, backup deorbit-2 slot is available i.e., one day after the nominal deorbit-2 plan, in order to meet the desired initial conditions for powered descent phase. Also approximately 24 h before powered descent initiation, trajectory correction maneuver slot is available, to correct the state deviations at the powered descent start, arising due to DEO-2 maneuver execution errors. However, these backup slot is not exercised during the Chandrayaan-2 mission because of the nominal performance of the de-orbit maneuvers.

10. Vikram powered descent trajectory design

Powered descent phase starts from the periselene of the transfer orbit phase when the lander's elliptical orbital track is going to pass over the desired site. The powered descent phase is split further into four phases due to various mission constraint as shown in Fig. 5.

First phase is named as *braking with rough navigation* and its objective is to break the lander's velocity suitably before a specified altitude for LPDC imaging. Phase 2 is named as *attitude hold* and as its name suggest the attitude of the lander is withheld at specified orientation for better imaging of the lunar surface. The goal of the phase 3, i.e. *braking with precise navigation* is to guide the lander to identified safe site as well as to reduce its kinetic energy and to orient the lander vertical which is necessary for landing. Finally, in vertical descent phase, the lander gradually descents vertically till the lander's legs touch the surface of the Moon.

10.1. Cost function selection

The spacecraft fuel consumption is to be minimized if it is to carry a enhanced payload mass for useful lunar explorations. So the cost function for the multi-phase soft landing optimal control problem is selected as minimization of propellant throughout the powered descent trajectory.

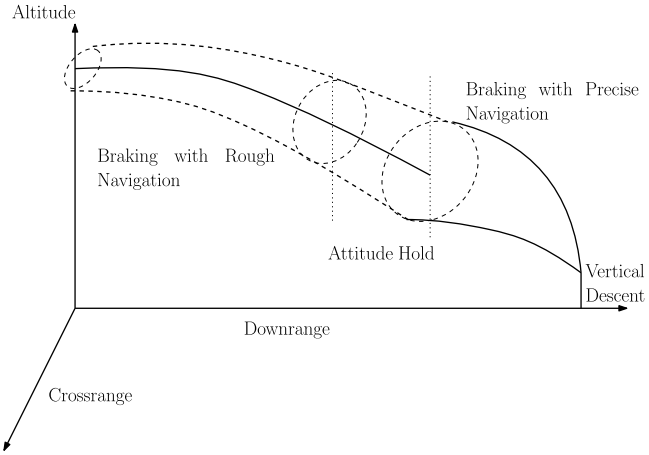

Fig. 5. Powered descent phase mission scenario.

10.2. Path/initial/terminal constraints

As the trajectory is segmented into a multi-phase trajectory, there are several constraints that are to be satisfied which are initial/terminal condition at each of the phases as well as path constraints along the phases.

10.2.1. Braking with rough navigation

This phase starts from the powered descent phase initiation conditions of post DEO-2 elliptical orbit at an altitude of approximately 30 km. The objective of this phase is to decrease the orbital velocity and to ensure terminal conditions with appropriate altitude and attitude for imaging. LPDC imaging capability determines the terminal altitude of this phase. Since image resolution improves as altitude decreases, ground test specifies an altitude upper limit below which the image resolution is better. Also, the lander's terminal attitude of this phase is specified based on the mounting angle of the LPDC and its field of view.

10.2.2. Attitude hold

The objective in this phase is to image the selected portion of the lunar surface, process it for the current location information so that in subsequent phase the guidance command guides the lander to the targeted safe landing site. Since there is not enough time for ground communication during landing, the image processing is carried out on Vikram's processor. The 'braking with rough navigation phase' specifies the initial conditions of this phase. It is to be noted that, at the terminal condition of 'braking with rough navigation phase', the lander is forced into a orientation of 50 deg for imaging subsequently by the LPDC. Throughout this phase, the thrust firing and attitude are held constant to avoid jittering during image capturing. Apart from LPDC, the absolute sensor LASA is used to get an altitude update during this phase.

Table 13
Terminal Condition (T.C.) for multi-phase landing problem.

Phase	Variables	Initial	Final
1	Vertical velocity	0	Free
	Tangential velocity	1.68 km/s	Free
	Across velocity	0 km/s	Free
	Altitude	30.4 km	7.4 km
	Thrust right ascension angle	Free	0 deg
	Thrust declination angle	Free	50 deg
2	Vertical velocity	Phase 1 T.C.	Free
	Tangential velocity	Phase 1 T.C.	Free
	Across velocity	Phase 1 T.C.	Free
	Altitude	Phase 1 T.C.	Free
	Thrust	Phase 1 T.C. $\forall t$	
	Thrust right ascension angle	0 deg$\forall t$	
	Thrust declination angle	50 deg$\forall t$	
3	Vertical velocity	Phase 2 T.C.	0
	Tangential velocity	Phase 2 T.C.	0
	Across velocity	Phase 2 T.C.	0
	Altitude	Phase 2 T.C.	400 m
	Thrust right ascension angle	Phase 2 T.C.	0 deg
	Thrust declination angle	Phase 2 T.C.	0 deg

10.2.3. Braking with fine navigation

At the terminal part of the 'attitude hold phase', the correct update of the position of the lander with respect to safe site is known i.e., downrange and crossrange information from the LPDC sensor and altitude information from the LASA sensor. The objective of the 'braking with precise navigation' is to guide the lander from the terminal condition of the 'attitude hold phase' to an altitude of 400 m above the landing site with zero kinetic energy. Further, in the terminal condition, the lander's orientation should be vertical, which favors the lander's legs to touch the Moon's surface.

For more details on the mathematical details of the powered descent ground trajectory design, interested reader can refer to [35–38].

10.3. Powered descent simulation results

Multi-phase lunar landing problem is formulated as optimal control problem and then converted into a nonlinear programming problem (NLP) using Legendre pseudospectral method [39]. The NLP solver uses sequential quadratic programming which solves a sequence of subproblems based on the quadratic model of the original problem [40]. The Lagrangian is constructed using the quadratic model with linear and non-linear constraints using Karush–Kuhn–Tucker necessary condition. The idea behind this approach is to model at the current iterated solution by quadratic programming subproblem, then use the minimizer of this subproblem to define a next iterated solution. The step size at every iteration is based on the lagrangian merit function with a linesearch method [41]. The difference between the current and previous iterated solution is checked for the tolerance specified. If the difference is less than the tolerances, the iteration stops otherwise the search continues in the descent direction calculated by sequential quadratic programming. The covector mapping principle eliminates the curse of solving the co-state vector associated with the optimal control problem. The optimality of the generated spectrally accurate solution is verified by Pontryagin's Minimum Principle.

Initial and final condition for the lander is provided in Table 13. In the formulation, these conditions are absorbed as constraints in the optimal control algorithm. As seen in Table 13, each phase has its own mission constraints. Phase 1 ('braking with rough navigation') terminal condition in altitude and attitude has been selected based on LPDC as explained in Section 10.2.1. Phase 2 ('attitude hold') constraint emphasizes on avoiding jittering during imaging. Phase 3 ('braking with precise navigation') constraints enforce soft vertical landing. Detailed description of these constraints has been discussed in the literature [35].

Table 14
Vikram powered descent uplinked strategy. PD Initiation (UT): 2019-09-06, 20:07:54:128.

Phases (MCMF-PA)	Altitude (km)	Latitude (deg)	Longitude (deg)
Rough braking	30.4	−51.434	22.887
Attitude hold	7.4	−70.623	22.806
Fine braking	5.2	−70.764	22.797
Hovering	1.3	−70.899	22.781
Touch down	0.9	−70.902	22.781

On 6th, September 2019 UT, 8 h before the powered descent initiation, the trajectory design has been carried out for uplinking the target milestones which in-turn has to be achieved by onboard guidance scheme. Fig. 6(a) shows the decreasing altitude profile of the lander satisfying all mission constraints i.e. first phase terminal constraint of 7.4 km and third phase terminal constraint of 400 m. Fig. 6(a) also shows the down range traced by the lander. Fig. 6(b) shows the cross range traced by the lander which is negligible since there is no cross range error with respect to the desired site. Figs. 6(c)–6(e) show the velocity components of the lander satisfying the mission constraints of soft landing.

Fig. 6(f) provides the demanded thrust throttling percentage for satisfying all the mission constraints given in Table 13. In attitude hold phase, since the throttling percentage and orientation is held constant, the vertical velocity components increases as shown in Fig. 6(d). In the subsequent braking with precise navigation phase, the throttling percentage and orientation is derived from the current states to achieve soft landing.

The thrust vector declination angle profile provided in Fig. 7(a) satisfying constraints viz., attaining terminal constraint of 50 deg at the 'braking with rough navigation phase' and 0 deg at the 'braking with precise navigation phase'. It is to be noted that in LVLH frame, the thrust vector declination angle is defined as the orbital in-plane angle of the thrust vector whereas thrust right ascension angle is defined as the orbital out-of-plane angle of the thrust vector. Fig. 7(b) shows the thrust vector right ascension angle satisfying terminal constraints. Note that in 'attitude hold phase', the throttling percentage and thrust declination as well as right ascension angle is maintained constant throughout as per the mission requirement.

Based on this design, target milestones in Moon centered Moon fixed principle axis (MCMF-PA) frame [23] have been worked out. A brief summary of the altitude and position to be achieved by closed loop guidance design during powered descent phase is tabulated in Table 14 which has been uplinked to the spacecraft 6 hrs before 2019-09-06, 20 : 07 UT.

After initiating the powered descent phase at the epoch mentioned in Table 14, *Vikram* is fully autonomous i.e., it is controlled by automatic landing sequencer for soft-landing. Irrespective of it, *Vikram* hard landed on the Moon surface. However, the ground trajectory design of the Chandrayaan-2 mission i.e., target lunar orbit design, launch opportunities design considering the launch vehicle constraints, Earth bound maneuver design, trans lunar injection, lunar orbit insertion, lunar bound maneuvers design, deorbit design lead to the success of achieving the desired lunar orbit which passes through the landing site at sunrise time satisfying all the mission constraints. It is to be noted that the challenges involved in Chandrayaan-2 orbit modeling, orbit determination and its comparison with realized orbit during the Earth bound and lunar bound phase is a subject of another paper in the near future.

11. Conclusion

Chandrayaan-2 mission is designed to expand the lunar scientific knowledge through detailed study of topography, seismography, mineral identification etc. In this paper, trajectory design — Earth phase,

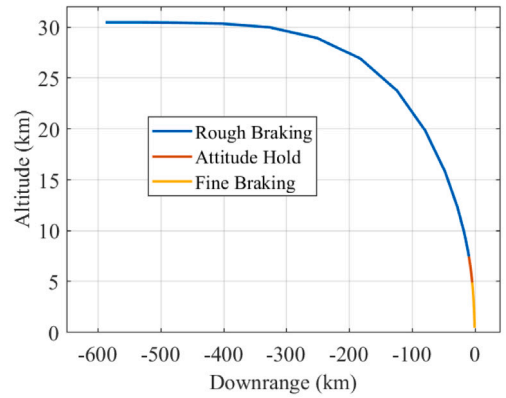

(a) Altitude and downrange trajectory during descent of the lander

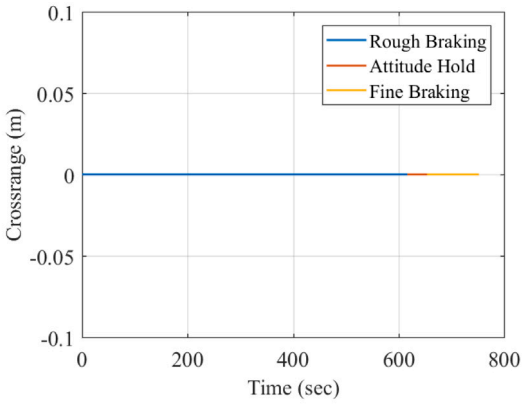

(b) Crossrange traced by the lander

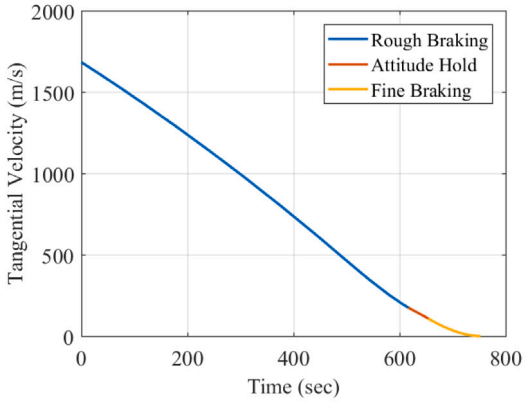

(c) Tangential velocity profile of the lander

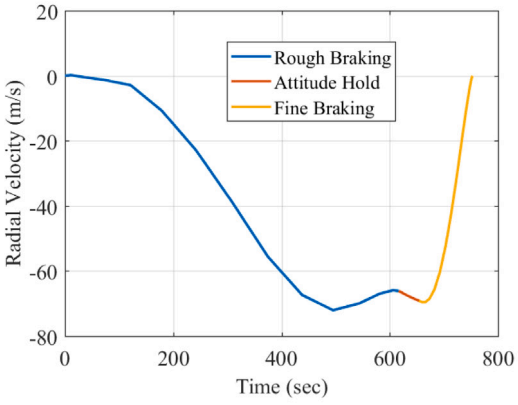

(d) Radial velocity profile of the lander

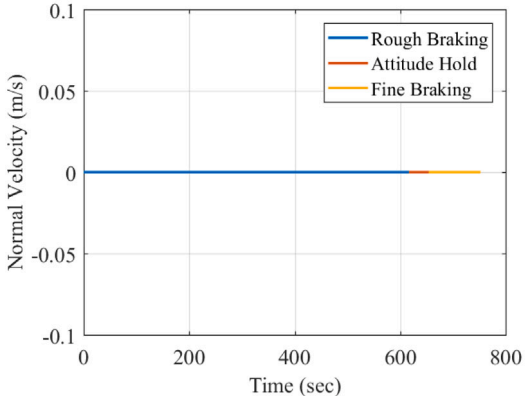

(e) Normal velocity profile of the lander

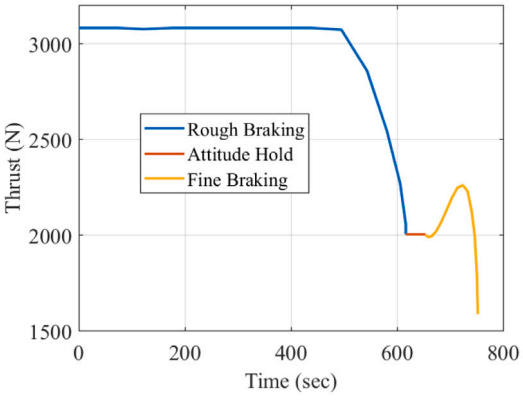

(f) Demanded thrust firing for achieving mission goals

Fig. 6. Multi-phase lunar landing ground trajectory solution.

transfer phase, lunar phase involving the finite maneuver burns, keeping in mind the mission constraints, has been explained for ISRO's first attempted lunar landing mission, Chandrayaan-2. The target lunar orbit has been designed on the basis of maximizing the mission life of lander by landing at the time close to sunrise and also to image the landing site when it is illuminated using OHRC payload before the start of powered descent phase. The major mission constraints are engine burns in the availability of ground stations, minimum eclipse duration in the composite lunar phase and minimum delta-V expenditure for the overall trajectory design. Consequently, EPO-AOP and lunar RAAN required to make the spacecraft pass through the desired site at the desired illumination epoch has been computed for every month starting from July–December 2019. Owing to the higher mass of spacecraft (around 4000 kg), launch vehicle GSLV Mark III has been chosen which can provide different AOP values for different apogee heights. Different launch opportunities of the Chandrayaan-2 spacecraft and the respective landing scenarios was worked out for various EPO options provided by GSLV. Among which, EPO corresponding to 178° AOP has been preferred from GSLV because of maximum apogee height. Based on all this analysis, the Chandrayaan-2 spacecraft has been launched

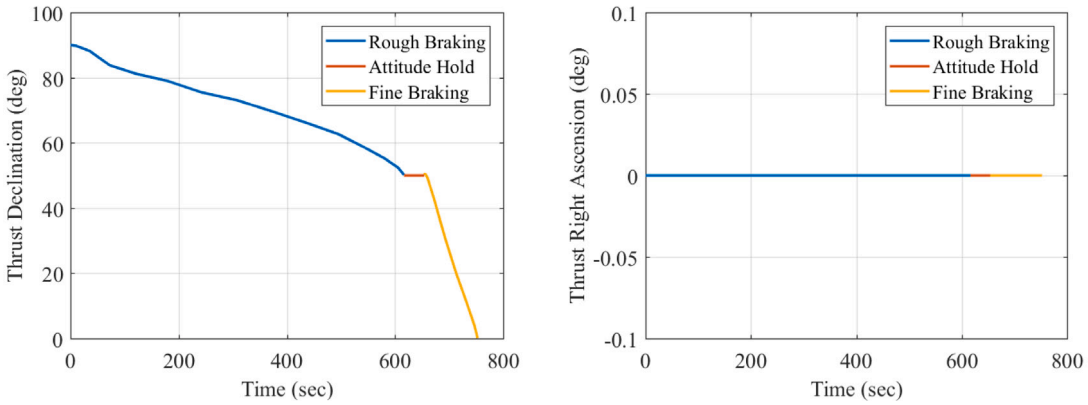

(a) Thrust declination angle profile ensuring vertical landing of lander

(b) Thrust right ascension angle profile ensuring vertical landing of lander

Fig. 7. Multi-phase lunar landing ground trajectory solution.

on 22nd July, 2019 UT and successfully rendezvoused with the Moon on 20th August, 2019 UT as planned.

Further, once the spacecraft has been inserted into highly elliptical orbit of 150×18000 km around Moon, four lunar burns (excluding LOI) are carried out to achieve the near circular 120 km orbit. Subsequently, the lander was separated on 2nd September 2019 UT following which two de-orbit burns are performed to maneuver the lander from 120 km circular orbit to 120×30 km elliptical orbit. Performance of every burn in Earth as well as lunar phase is nominal and has been tabulated in this paper along with post realized orbital details. Finally, the powered descent trajectory design is carried out and the phase is initiated from 120 × 30 km orbit on 6th September 2019 UT for soft-landing. Hence the overall ground trajectory design presented in this paper leads to the success of achieving the target lunar orbit and subsequently the desired landing site accurately for the Chandrayaan-2 spacecraft.

Declaration of competing interest

The authors declare that they have no known competing financial interests or personal relationships that could have appeared to influence the work reported in this paper.

Acknowledgments

The authors are thankful to the Indian Space Research Organisation (ISRO) for giving an opportunity to work on this challenging problem. Also thankful to colleagues of ISRO as well as Jet Propulsion Laboratory, NASA for their technical support during the Chandrayaan-2 mission.

References

[1] J.M. Sarkissian, Return to the Moon: A sustainable strategy, Space Policy 22 (2) (2006) 118–127.
[2] L. Taylor, G. Kulcinski, Helium-3 on the Moon for fusion energy: the Persian Gulf of the 21st century, Solar Syst. Res. 33 (1999) 338.
[3] H. Benaroya, L. Bernold, Engineering of lunar bases, Acta Astronaut. 62 (4–5) (2008) 277–299.
[4] J. Hickman, H. Curtis, G. Landis, Design consideration for lunar based photovoltaic power systems, in: IEEE Photovoltaic Specialists Conference, 1990, pp. 1256–1262, http://dx.doi.org/10.1109/PVSC.1990.111815.
[5] M.B. Duke, W.W. Mendell, B.B. Roberts, Strategies for a permanent lunar base, in: Lunar Bases and Space Activities of the 21st Century, 1985, p. 57.
[6] D. Dunham, R. Farquhar, N. Eismont, E. Chumachenko, S. Aksenov, A. Genova, J. Horsewood, R. Furfaro, J. Kidd, Using lunar swingbys and libration-point orbits to extend human exploration to interplanetary destinations, in: 64th International Astronautical Congress, Vol. 3, 2013, pp. 1932–1941.
[7] D. Schulze-Makuch, P. Davies, Destination mars: Colonization via initial one-way missions, J. Br. Interplanet. Soc. 66 (2013) 11–14.
[8] C. Pieters, J. Goswami, R. Clark, M. Annadurai, J. Boardman, B. Buratti, J. Combe, M. Dyar, R. Green, Character and spatial distribution of OH/H_2O on the surface of the Moon seen by M^3 on Chandrayaan-1, in: Science, Vol. 326, (5952) American Association for the Advancement of Science, 2009, pp. 568–572, http://dx.doi.org/10.1126/science.1178658.
[9] Q. Wang, J. Liu, A Chang'e-4 mission concept and vision of future Chinese lunar exploration activities, Acta Astronaut. 127 (2016) 678–683.
[10] T.J.W. Lazio, R. MacDowall, J.O. Burns, D. Jones, K. Weiler, L. Demaio, A. Cohen, N.P. Dalal, E. Polisensky, K. Stewart, et al., The radio observatory on the lunar surface for solar studies, Adv. Space Res. 48 (12) (2011) 1942–1957.
[11] R. Furfaro, B. Gaudet, D.R. Wibben, J. Kidd, J. Simo, Development of non-linear guidance algorithms for asteroids close-proximity operations, in: AIAA Guidance, Navigation, and Control (GNC) Conference, 2013, p. 4711.
[12] V.A. Chobotov, Orbital Mechanics, American Institute of Aeronautics and Astronautics, 2002.
[13] E.E. Macau, Using chaos to guide a spacecraft to the moon, Acta Astronaut. 47 (12) (2000) 871–878.
[14] K.C. Howell, M. Kakoi, Transfers between the Earth–Moon and Sun–Earth systems using manifolds and transit orbits, Acta Astronaut. 59 (1–5) (2006) 367–380.
[15] X. Ming, X. Shijie, Exploration of distant retrograde orbits around Moon, Acta Astronaut. 65 (5–6) (2009) 853–860.
[16] J.S. Parker, R.L. Anderson, Low-Energy Lunar Trajectory Design, Vol. 12, John Wiley & Sons, 2014.
[17] R. Biesbroek, Lunar and Interplanetary Trajectories, Springer, 2016.
[18] MS windows NT Kernel description, 2020, https://directory.eoportal.org/web/eoportal/satellite-missions/c-missions/chandrayaan-2, (Accessed: August 2020).
[19] B.K. Prasad, G. Kashvap, K. Muralidhara, J.S. Rao, A. Sharma, B. Sudha, S. Padmasree, et al., High accuracy star sensor for Indian regional navigational satellite segment NAVIC, in: 2018 Second International Conference on Electronics, Communication and Aerospace Technology, ICECA, IEEE, 2018, pp. 1271–1274.
[20] M.J. Sidi, Spacecraft Dynamics and Control: a Practical Engineering Approach, Vol. 7, Cambridge university press, 1997.
[21] MS windows NT kernel description, 2020, https://www.isro.gov.in/chandrayaan2-payloads, (Accessed: August 2020).
[22] J.N. Goswami, M. Annadurai, Chandrayaan-1 mission to the Moon, Acta Astronaut. 63 (11–12) (2008) 1215–1220.
[23] MS windows NT kernel description, 2020, https://lunar.gsfc.nasa.gov/library/LunCoordWhitePaper-10-08.pdf, (Accessed: August 2020).
[24] MS windows NT kernel description, 2020, https://www.iau.org/news/announcements/detail/ann18010/, (Accessed: August 2020).
[25] MS windows NT kernel description, 2020, https://ssd.jpl.nasa.gov/ephemerides, (Accessed: August 2020).
[26] MS windows NT kernel description, 2020, https://www.isro.gov.in/launcher/gslv-mk-iii-m1-chandrayaan-2-mission, (Accessed: August 2020).
[27] MS windows NT kernel description, 2020, https://www.isro.gov.in/launchers/gslv-mk-iii, (Accessed: August 2020).
[28] MS windows NT kernel description, 2020, https://en.wikipedia.org/wiki/Satish_Dhawan_Space_Centre, (Accessed: August 2020).
[29] MS windows NT kernel description, 2020, https://ccmc.gsfc.nasa.gov/models/modelinfo.php?model=DTM, (Accessed: August 2020).
[30] MS windows NT kernel description, 2020, https://ccmc.gsfc.nasa.gov/modelweb/atmos/jacchia.html, (Accessed: August 2020).
[31] H.D. Curtis, Orbital Mechanics for Engineering Students, Elsevier, 2010.

[32] J.K. Miller, E.A. Belbruno, A method for the construction of a lunar transfer trajectory using ballistic capture, in: Spaceflight Mechanics 1991, 1991, pp. 97–109.
[33] J.E. Prussing, Simple proof of the global optimality of the Hohmann transfer, J. Guid. Control Dyn. 15 (4) (1992) 1037–1038.
[34] A. Graphics, Inc (AGI) Systems Tool Kit (STK), AGI Product Literature, 2020, https://www.agi.com/products/stk, (Accessed: August 2020).
[35] S. Mathavaraj, R. Pandiyan, R. Padhi, Constrained optimal multi-phase lunar landing trajectory with minimum fuel consumption, Adv. Space Res. 60 (11) (2017) 2477–2490.
[36] S. Mathavaraj, R. Padhi, Explicit constrained terminal acceleration optimal guidance for three dimensional lunar landing, in: AIAA Guidance Navigation Control Conference, 2017, pp. 1267–1279, http://dx.doi.org/10.2514/6.2017-1267.
[37] S. Mathavaraj, R. Pandiyan, R. Padhi, Optimal trajectory planning for multiphase lunar landing, in: Advances in Control and Optimization of Dynamical Systems, Vol. 49, (1) Elsevier, 2016, pp. 124–129.
[38] S. Mathavaraj, R. Pandiyan, N. Ghatpande, N. Gopinath, A predictive guidance scheme for soft landing of a lunar module, in: 63rd International Astronautical Congress, IAF, 2012, pp. 1–12.
[39] I. Ross, A Beginner's Guide To DIDO: A MATLAB Application Package for Solving Optimal Control Problems, Technical Report, 2007, Elissar, TR-711.
[40] I. Ross, F. Fahroo, Pseudospectral knotting methods for solving nonsmooth optimal control problems, in: J. Guid. Control Dyn., Vol. 27, (3) 2004, pp. 397–405, http://dx.doi.org/10.2514/1.3426.
[41] J. Nocedal, S.J. Wright, Sequential Quadratic Programming, Springer, 2006.